

## A CASE STUDY IN COMPONENT REDESIGN FOR ADDITIVE MANUFACTURING PROCESS WORKFLOWS

Elliott Jost\*, Jaime Berez\*, Christopher Saldaña\*

\*George W. Woodruff School of Mechanical Engineering, Georgia Institute of Technology, 801  
Ferst Drive NW, Atlanta, GA 30332

### Abstract

Additive manufacturing (AM) has matured beyond limited use-cases in rapid prototyping into a process capable of competing with conventional manufacturing methods in the production of end-use components. As such, many manufacturers are evaluating candidate products for redesign for AM, with interest in improving component performance, streamlining manufacturing, and reducing costs. In this study, the authors argue for systematic use of opportunistic design tools such as generative design and for the inclusion of restrictions imposed by the entire manufacturing process workflow to be included in the design process. Emphasis is placed on how secondary processing steps, that is, those other than the primary AM process, inform design. A bicycle stem is used as an exemplar case study of component redesign for AM. Generative design is used to optimize the component's weight given the design constraints. An end-to-end manufacturing process chain is consequently developed and analyzed for viability, covering design for additive manufacturing (DFAM) and post processing. Through this comprehensive case study, it is shown that significant weight savings, greater than 25% in the present case, can be achieved through the DFAM process. Guidelines from the DFAM process are generalized for application to further cases.

### Introduction

Additive manufacturing (AM) has shifted the manufacturing and design paradigm in recent years, particularly as some AM technologies have matured from rapid prototyping methods to suitability for production-scale manufacturing. Laser powder bed fusion (LPBF) is an AM technology which can process metals by using a laser heat source to fuse selective areas in a thin bed of metal powder feedstock, repeated in a layer-wise manner, progressively building the workpiece. Of the currently available metal AM processes, LPBF has been rapidly commercialized and has been adopted within industries such as aerospace to medical which utilize LPBF for near-net-shape manufacturing of relative dense geometrically complex components. Additive manufacturing favored in large part because of the significant design freedom it offers, as has been reported [1]. Along with this newfound design freedom comes a significant shift in how designers conceptualize designs, think about redesign of components and assemblies, and utilize tools for design improvement or optimization. In the present work, the authors argue that the successful design for AM (DFAM) workflow incorporates considerations spanning the entire manufacturing process chain, and that post-processing manufacturing technologies are a crucial, yet commonly neglected aspect of the DFAM process. In the ensuing, a case study is presented in which a bicycle stem formerly manufactured via conventional means is redesigned for LPBF AM. Evaluation of design tradeoffs relating to the entire manufacturing process chain are considered and discussed.

Design for additive manufacturing (DFAM) has been an object of study since AM technologies were recognized to enable “free complexity” in design [1–4]. Laverne et al. [5] divided DFAM into two categories for design assessment: opportunistic and restrictive design, which will be discussed and applied in the context of the present study. Opportunistic design is a design methodology which emphasizes utilization of the geometric and material complexity offered by AM to improve designed components and manufacturing workflows. This includes but is not limited to advanced design and optimization technologies such as topology optimization (TO) and generative design (GD), each of which utilizes computational algorithms to provide improved designs. Conversely, the restrictive DFAM methodology focuses on using the limits of AM such as natural constraints relating to minimum manufacturable feature size, surface finish, or the manufacture of overhanging structures to guide the design workflow. Meisel et al. [6] argued that a successful design utilizes both opportunistic and restrictive design, which is referred to as dual design. Similarly, Hällgren et al. [7] divided the DFAM into process and designer driven, incorporating software tools and human experience into the design process. In process driven DFAM, a focus is put on manual interaction to reduce design time. This can incorporate complex technologies such as TO and GD, as mentioned above. Designer driven DFAM utilizes more simplistic, less deterministic methods. For example, a designer may use lattices to reduce mass on an object as opposed to a more complex topology optimization implementation.

Opportunistic, computer-aided design tools such as TO or GD are being increasingly relied upon because of their ability to maximize the potential of AM [8]. Despite this, these software tools are not yet well integrated into design and manufacturing workflows [9]. TO and GD provide systematic, rigorous, and mathematical exploring of large design spaces. Topology optimization has been widely studied [10–13] for AM, and utilizes mathematical optimization to converge on optimal designs given an objective function, typically defined as a displacement, structural load, or thermal performance, and a complimentary set of boundary conditions. Similarly, GD, a relatively new design tool enabled by computing power increases in recent years, uses artificial intelligence to create suggested designs that optimize for a specific objective. These tools are useful because, as Wu et al. [14] writes, “even for the most experienced designers, their intuition might be limited when manually exploring” a design space. Despite the use of both TO and GD in exploring large design spaces, these tools must be used responsibly, and do not currently incorporate all necessary design considerations, as will be demonstrated in the present paper.

Despite claims that AM can create fully functional end-use components [6,15], the authors argue that this is the exception and not the rule. Although AM processes, and specifically LPBF, can create end-use components in their as-printed condition in certain scenarios, it is much more common to require significant post-processing. Peng et al. [16] similarly argued that AM faces critical issues inhibiting the direct use of as-printed parts. Example scenarios which require significant post-processing include fatigue applications [17–19] and interface surfaces, each of which is well documented in the literature. Manufacturing methods used in these scenarios may include heat treat [20,21], hot isostatic pressing (HIP) [22–24], and surface finishing [25–28]. Consequently, the authors posed that successful DFAM incorporates all aspects of the manufacturing process chain and is not limited to considerations related only to the AM process to be used. This conclusion is consistent with multiple reviews covering topics within DFAM that similarly agree that manufacturing considerations should be further incorporated into the DFAM workflow [5,29–31], and is demonstrated explicitly through the case study redesign in the present

work. Furthermore, restrictive design should consider constraints on manufacturing freedom imposed by AM, but also by the subsequent manufacturing technologies used for post-processing necessary to create an end-use component. In the present study, a case example part - a bicycle stem component - is redesigned using both opportunistic and restrictive DFAM strategies with emphasis on the post-processing strategies necessary to fully implement such a component.

### **Redesign approach**

In this work, the application of a dual design approach to DFAM is utilized, with an emphasis on how manufacturing processes beyond the AM process supply restrictive input to the design process. That is to say, incorporating manufacturing process planning considerations into design stages (embodiment and detail design) is vital. As is well established by the literature, opportunistic DFAM approaches such as GD should be incorporated in embodiment design to reap the benefits which AM can provide [5,6]. Additionally, heuristics for DFAM need to be applied as restrictions to ensure manufacturability. Here, it is emphasized that AM processes for metals such as LPBF are rarely the sole manufacturing process required to produce a functional product. The LPBF process is well understood to produce geometry with poor dimensional control [32], gross deformation due to residual stress, high surface roughness [33], low microstructural heterogeneity [34], and high volumetric defect content [35]. As such, secondary manufacturing processes are often leveraged to address these shortcomings [16]. Further, the sequence of secondary processing steps suitable to an AM component may be product- or application-specific and does not necessarily mirror classical approaches to manufacturing process planning. The design process must incorporate this knowledge from an early stage for the DFAM approach to supply viable and competitive alternatives to conventional manufacturing workflows.

Figure 1 shows the proposed workflow for DFAM. At top, the overall design process is coarsely shown, which includes problem definition, conceptual design, embodiment design, and detail design [5,36]. The additional step of manufacturing process planning has been added, which is connected by arrows to various stages of the design process to emphasize the iterative nature of the design process and post-processing considerations necessary for consideration in the design. Note that while this step is shown to be strictly outside of the design process as classically defined, this work argues for its close relation. Several of these high-level steps are enclosed within a dotted box, and these steps are expanded upon in detail in the middle portion of the figure. Since the case study presented is for a relatively simple component-level redesign, the conceptual design step is not emphasized. Rather, embodiment and detail design are focused on. These stages are expanded upon in the chart, and are comprised of configuration & parametric design, DFAM, simulation & down selection, and design for manufacturing (DFM). DFAM is shown as informing configuration and parametric design (note the left-pointing arrows) based on dual inputs: opportunistic and restrictive. Opportunistic inputs might support the selection of a GD design with organic and complex geometries, for example. Restrictive inputs will inform material selection, the minimal feature size, or the design of self-supporting geometry, for example. The incorporation of these DFAM principles is iterative, as illustrated below by the loop formed in the flow chart. Simulation and down selection follows as a highly flexible step which may vary on a case-by-case basis. Simulation may be performed to validate a GD design, test the robustness of a design against a variety of parametrically changed loading scenarios, or test performance in the presence of small design modifications. Down selection between multiple GD designs or lattice variations may also

be required. DFM is a subsequent step which informs all prior steps. Here, designers must acknowledge in detail the likely necessity of secondary processing steps and incorporate these considerations iteratively. Finally, at the lower portion of the figure, a generalized manufacturing process workflow where AM is the primary process, is shown. The intimate and detailed knowledge of the manufacturing process workflow undergirds the DFAM and DFM steps, shown via the dotted arrows.

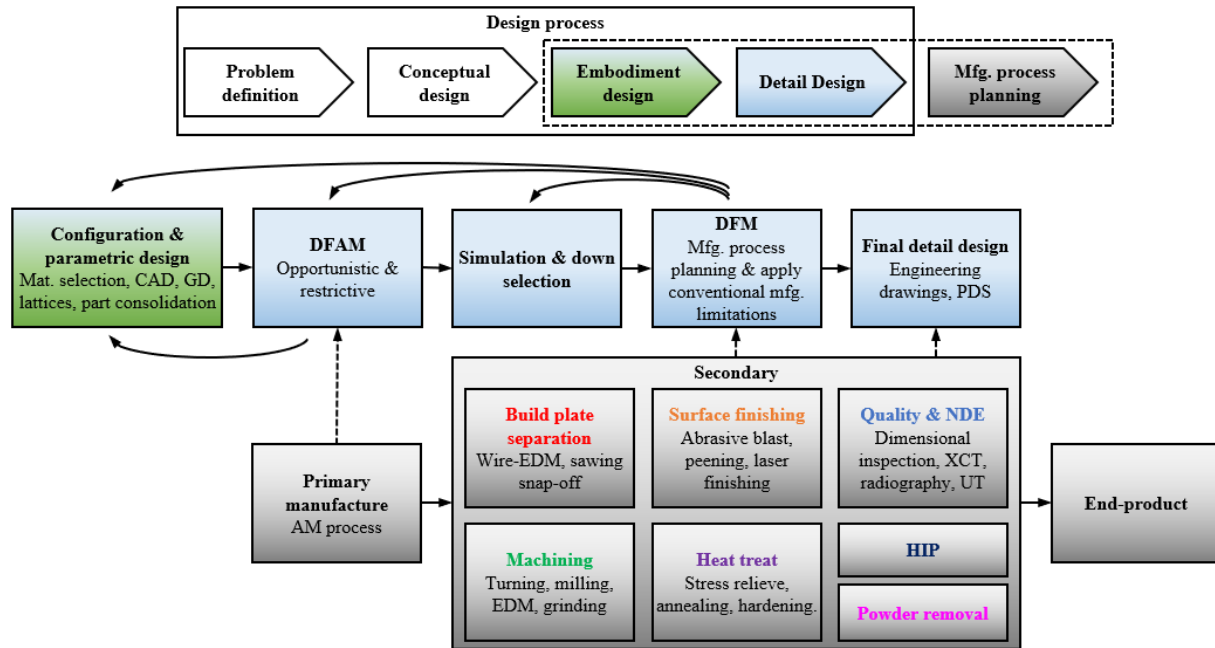


Figure 1. Generalized AM design and manufacturing process planning workflow.

In the lower portion of Figure 1, which encompasses manufacturing process planning, the primary manufacturing process, AM, feeds into an unordered set of potential secondary processes. Some of these processes are semi-specialized to AM or even the selected AM process, such as build plate separation or HIP. Others are more common secondary steps in manufacturing workflows, such as machining, heat treat, surface finishing, or quality and non-destructive evaluation (NDE). Even so, there are still AM-specific considerations to be addressed. Surface finishing may take on greater importance and require novel approaches due to the characteristically rough surfaces produced by AM [32,33]. Quality and NDE steps such as X-ray computed tomography (XCT) may be essential due to the defect prone nature of AM [34,35,37] and complex geometries difficult to inspect via traditional methods. Stress relief, as a heat treat operation, may be required more frequently for AM parts than is typical. Machining may tend to leverage certain processes such as EDM due to its nature as a zero-force machining method appropriate for delicate geometries and insensitivity to high hardness, low-machinability materials popular for use with AM such as stainless steels, nickel- and cobalt-based super alloys, and refractory metals [38,39]. Finally, the ordering of each of these steps will likely be specific to the material, geometry, AM technology, and design application considered. This ordering will be further discussed in the subsequently presented case study.

An exhaustive list of secondary processing concerns for AM products would be out of scope for a single study. In addition to the generalized explanation above, this work presents a case study which illustrates specific examples of how a design process for additively manufactured products requires not only DFAM principles but supporting DFM principles. Critically, these considerations are specific to the integration of AM in a larger manufacturing process plan.

### Case study

To better understand and illustrate the DFAM process as discussed above, a bicycle stem was chosen as an exemplar part to be redesigned. A bicycle stem serves as the connection between the steerer tube on the front fork and the handlebars, as shown in Figure 2. A bicycle stem is intended to be lightweight yet stiff to provide the rider with efficient control of the handlebars. Thus, the objective of the case study is to redesign a traditional bicycle stem for AM with the goal of minimizing weight while still meeting the design requirements.

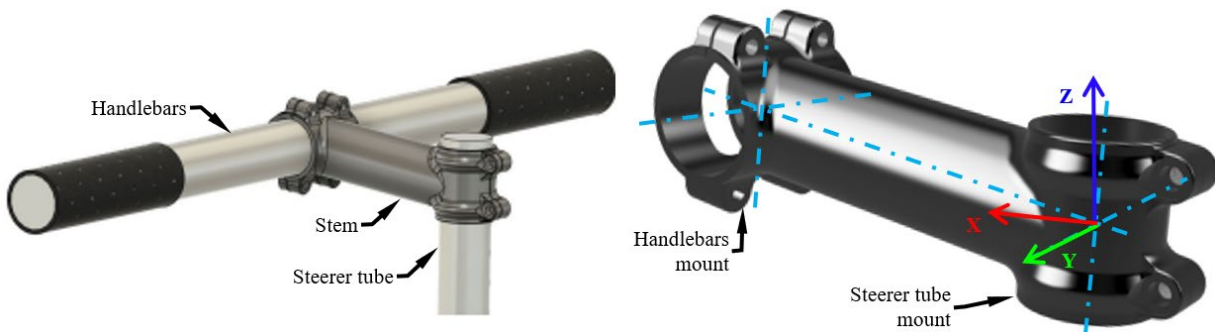


*Figure 2. Bicycle stem schematic description.*

### **Problem definition: Design constraints**

Service requirements in the form of loading conditions were determined through a literature search of loads experienced on a bicycle during common riding scenarios [40,40,41]. Three categories of scenarios were identified including starting, braking, and hitting a pothole. Loads corresponding to these scenarios are detailed in Table 1 below. Starting 1 and 2 are mirror images of each other because of the asymmetric loading experienced during the start depending on whether the rider begins with force on the left or right pedal. The loading conditions were adapted to represent those experienced for a 90 kg (200 lbs) rider. The force and moment directions noted correspond to the coordinate system used in Figure 2, where the Z direction is vertical, X is along the forward movement direction of the bicycle, and Y is mutually perpendicular. Note that the stem has a tilt of 5° from the X direction, as seen in Figure 2, which is common practice to improve the ergonomic position of the handlebars.

*Table 1. Bicycle stem loading conditions for 90 kg rider*

	Force (N)			Moment (N·m)		
	$F_x$	$F_y$	$F_z$	$M_x$	$M_y$	$M_z$
<b>Starting 1</b>	-174	-58	417	-211	0	-19
<b>Starting 2</b>	-174	58	417	211	0	19
<b>Braking</b>	448	0	-172	0	0	0
<b>Pothole</b>	500	0	-1250	0	0	0

## Embodiment design

In-depth conceptual design was not emphasized for this case study since the existing conceptual design for a bicycle stem is well defined. Furthermore, because the present case study is a redesign of an already existing product, this work's focus has been put on the later stages of the design process. As such, this case study begins with embodiment design. Embodiment design as defined in Figure 1 includes material selection, early CAD product definition, and GD optimization, each of which are discussed below.

### Material selection

Because weight is to be minimized in this redesign, a high specific property material is desirable. In other words, materials with high stiffness or strength on a per weight basis are desired. Early conceptual design identified metal alloys as the candidate material class for this design. Non-structural alloys, e.g., copper alloys, tool steels, precious metals, refractory alloys, were also excluded in early conceptual design. At the embodiment design stage, a process-first approach to material selection was used, providing restrictive DFAM input to the design process. Materials compatible with the LPBF process were considered, restricted to those which are commercially available in suitable powder form from multiple suppliers, including prevalent ferrous alloys, e.g., stainless steel 17-4 and 316, non-ferrous alloys, e.g., aluminum AlSi10Mg and titanium Ti-6Al-4V, and super alloys, e.g., Inconel 718. Material selection was performed using material performance indices in the form of Ashby charts. The indices selected were  $\sigma_y/\rho$  and  $E/\rho$ , where  $\sigma_y$  is yield strength,  $E$  is the modulus, and  $\rho$  is the material density. Ashby charts which plot modulus and yield strength against density are shown in Figure 3. These indices identify the most mass-efficient material to maximize strength and stiffness for a tensile loading application. While the stem is subject to applied forces which create net bending and torsion, the developed GD geometry has strut-like geometrical elements which are primarily loaded in tension. This provides an interesting example of how opportunistic DFAM prompts different material selection approaches than conventional manufacturing. Should a design, such as that shown in Figure 2, be considered, material selection indices such as  $\sigma_y^{2/3}/\rho$ ,  $G^{1/2}/\rho$ , and  $E^{1/2}/\rho$  may be more appropriate to identify the most mass-efficient material for torsion and bending [36].

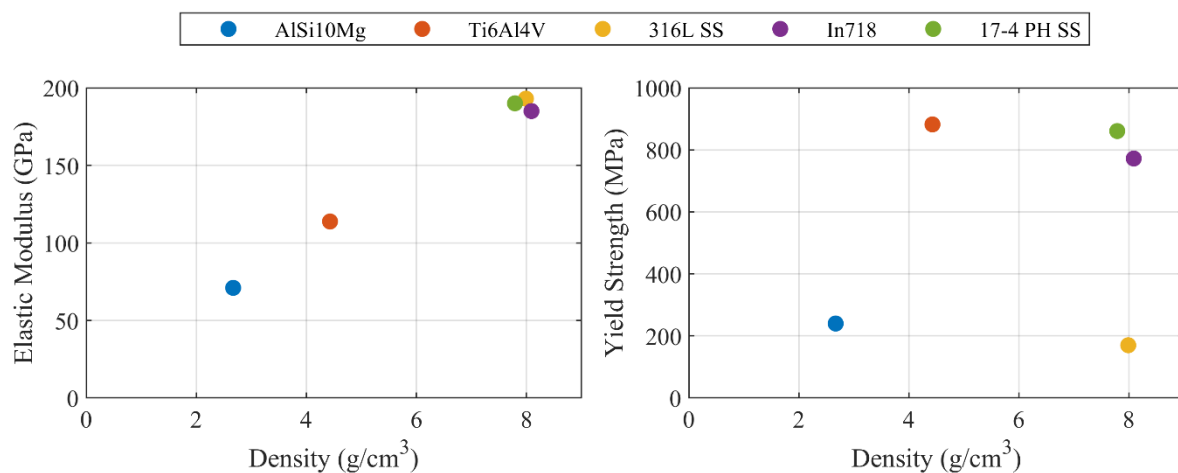


Figure 3. Ashby charts used for material selection

As shown in Figure 3, of the commercially available alloys suitable for the LPBF process, AlSi10Mg and Ti6Al4V (Ti64) have similar specific moduli at  $26.6 \times 10^6 \text{ m}^2/\text{s}^2$  ( $\text{Pa}/[\text{g}/\text{cm}^3]$ ) and  $25.7 \times 10^6 \text{ m}^2/\text{s}^2$ , respectively. However, Ti64 has by far the highest yield strength per density value of  $199 \times 10^6 \text{ m}^2/\text{s}^2$ . Consequently, Ti64 was selected as the material for use in this study.

### Generative design optimization

Generative design, a category of tools utilizing artificial intelligence to create optimized designs, has been chosen to augment the human designer's capabilities. Specifically, *Autodesk Fusion360* Generative Design was used in the present redesign to reduce the mass of the bicycle stem. To reduce the computational time, a simplified model of the bicycle stem without fillets, bolt holes, etc. was utilized. This had the additional advantage of creating a more design-agnostic bicycle stem model that did not assume a particular way of fixturing the bicycle stem to the handlebar and steerer tube. For the GD tool, volumetric regions of the design needed to be assigned to one of three categories: preserve, obstacle, or starting, as shown in in Figure 4(a). Preserve geometries are those regions that should not be acted upon by the GD tool such as mating surfaces, connections, etc. Starting geometry provides a reference point for the GD tool to begin designing from and is heavily influential on the converged upon designs, though its effects are not studied here. Obstacle geometry was placed in regions occupied by mating components, namely the handlebars and steerer tube.

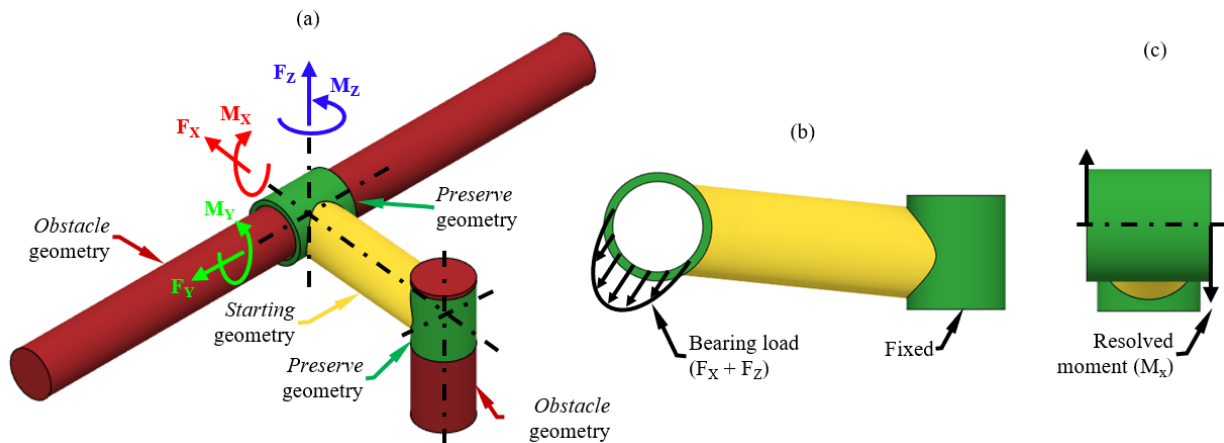


Figure 4. (a) Design space region categorization additionally showing a generalized case applied loads on the handlebar mount. (b) Side view showing an example of an applied bearing load on the handlebar mount. (c) Front view showing an example of a resolved moment on the handlebar mount.

Loads were applied within the GD tool using the built-in software tools. The inner surface of the steerer tube mount was fixed in all degrees of freedom. To simulate the application of loads as realistically as possible, the forces were applied as bearing loads, which have approximately parabolic force distributions, as illustrated in Figure 4. Moments were modified to be applied as forces at the edges of the handlebar mounts due to limitations in the application of moments within the software. Load cases were applied as individual scenarios within the GD tool, however the

software factors in all scenarios in proposed designs. An example of how various bearing loads or moments would be applied is illustrated in Figure 4(b-c).

In addition to design space categorization and load cases, the GD tool required inputs for the design objective, print orientation, maximum overhang angle, material properties, minimum feature thickness, and safety factor. The objective was set to minimize mass. Minimum feature thickness was set to 1.5 mm and maximum overhang angle to 45 degrees based on the known performance of the EOS M280, which was the exemplar commercial LPBF platform selected for this case study. Print orientation was specified as the +X direction as defined Figure 4. The material properties used corresponded to the Ti64 parameters shown in Figure 3. The safety factor was set to 2.0, where exceeding the yield strength of 881 MPa was the service criterion.

Based on the four load cases applied to the model and the requirements described above, the GD software generated several models that met the specified loading and manufacturing criteria. These designs were evaluated based on their weight savings and manufacturability. The chosen design is shown in Figure 5a, and was selected due to the significant weight savings through optimized material location. It should be noted that this intermediate design includes no integration of attachment points, or other general DfAM principles beyond the maximum overhang angle and minimum feature size constraints input to the GD software. Using the intermediate design shown above, the simplistic handlebar and steerer tube mounts were modified to include the bosses for pinch bolts as in the original design. In later manufacturing steps, both the handlebar and steerer tube mounts are split in a machining operation, thereby allowing the pinch bolts to apply clamping force. This modified design is shown in Figure 5b.

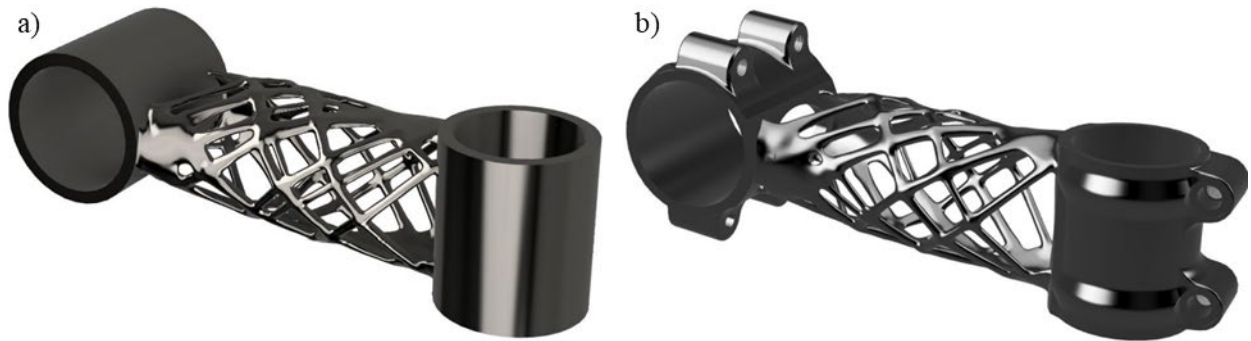


*Figure 5. (a) Intermediate bicycle stem design as output from the GD software tool. (b) Design as-modified to have bolt holes and attachment points as in the original stem design.*

### **Detail design**

The detail design phase of the design process includes detailed DFAM specific to the intermediate, embodiment design presented above in Figure 5. Specifically, considerations for limitations of the process, ease of manufacture, and preparation for secondary processing are discussed.

*Design for Additive Manufacturing*

Once the GD step was complete, DfAM considerations could be incorporated in further detail. This was done by evaluating the design shown in Figure 5b and making appropriate modifications to improve manufacturability for quality, speed, and ease. As specified in the generative design tool, the choice was made that the build direction would be parallel to the axial direction of the stem. With this part orientation, 20 build stems will be able to be made on a single 250 x 250 mm build area, the maximum build area of the EOS M280. Table 2 shows several DfAM heuristics that were considered and implemented. Discussion of tradeoffs and further considerations are presented below.

*Table 2. DfAM heuristics and resulting solutions*

<b>DfAM Heuristic</b>	<b>Solution/Implementation</b>
Features should be <1.5 mm for reliable process performance and geometrical control	Enforce through generative design tool
Horizontal holes must be < 8mm diameter	Add teardrop profile to circular bores above this size
Parts should be firmly attached to buildplate to sink heat and resist thermal deformation	Volumetric support added to bottom of steerer tube mount
Overhangs must be less than 45 degrees (from build direction)	Bolt hole boss modification, anchoring support on steerer tube mount
LPBF as-built surface texture not acceptable for mating surfaces	Add machining allowances to critical mating surfaces.
Minimize height to reduce build time	Favor more parts per build rather than reduced build time
The use of fewer supports reduces post-processing time	Remove need for supports where possible

Due to constraints input to the GD tool, the selected design meets the minimum feature size requirements. Furthermore, the previously selected build direction orients the struts or ligaments of the design at an acceptable build orientation to not require supports. The output of the GD tool is shown in stage 1 of Figure 6. This design was modified to include additional functional features in a detail design stage, as seen in stage 2 of Figure 6. As already discussed, bosses for pinch bolts were added. Additionally, the clamps were split across these bosses to enable the pinch bolts to properly function. This stage of design represents an early engineering product definition, as it might be used ‘in-service’ on the bicycle.

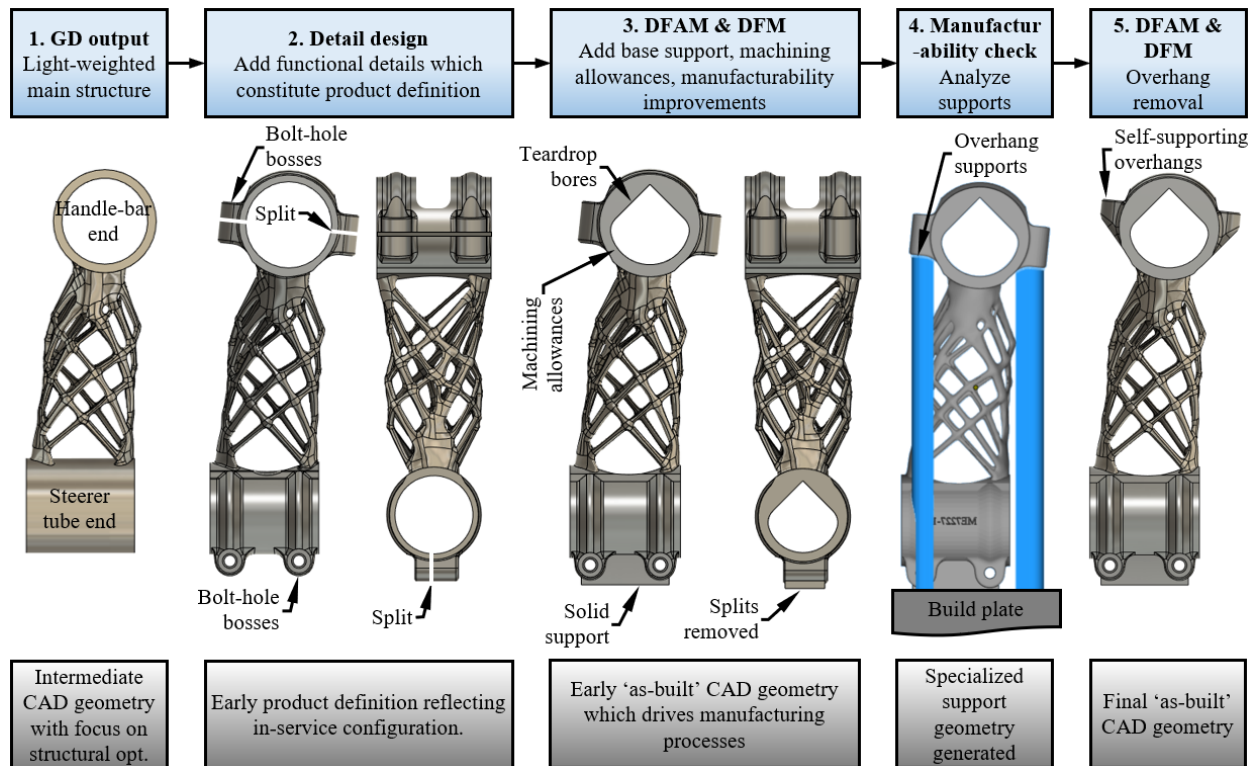


Figure 6. DFAM and DFM process.

Further evolution of this geometry is required to develop an ‘as-built’ design suitable for subsequent manufacturing steps – seen in stage 3 of Figure 6. As with all LPBF parts, the bicycle stem will need to be anchored to the build plate. For simplicity and ability to sink heat away from the part, a simple projected area solid volume support has been added. This support geometry will also provide allowance for separating the component from the build plate and will be removed in the finish machining process. A tradeoff of the selected build orientation is that the large bores on the handlebar and steerer tube mounts are oriented horizontally, and thus cannot be directly printed. To address this, the bores were modified to have a ‘teardrop’ profile, which prevents any internal surface from having an overhang greater than 45 degrees. A radial machining allowance of 1.25 mm was added to the bores as well so that the surface finish requirements can be met for the mating between the mounts and opposing surfaces. Diametrical allowances of 1.0 mm were added to the bolt holes to allow for drilling and tapping the holes to the proper requirements. Finally, the splits on the clamps were removed. The split on the handlebar clamp (top of the figure) cannot be integrated into the LPBF process, as it produces overhanging and floating geometry. While the steerer tube clamp split (bottom of the figure) could be manufactured with LPBF, it is also removed. This is due to a DFM consideration. The inner surface of the clamp must be finish-machined (discussed in detail later) and the presence of the split would prevent rigid work holding and produce chatter in cutting.

After this round of DFAM- informed design, a manufacturability analysis, seen in stage 4 of Figure 6, was performed using the software tool *Materialise Magics*, which is used to design supports and otherwise prepare files for AM. This analysis showed that the supports required to build the handlebar mount bolt hole bosses would be significant in size, intersect other stem geometry, and be difficult to remove in post-processing. As such, the DFAM process was repeated

iteratively, resulting in the geometry shown in stage 5 of Figure 6. Modifications were made to the bolt holt bosses, angling them such that supports were not needed. This results in final as-built CAD product definition, previously based on two intermediate models. This product definition has incorporated major restrictive DFAM considerations, after originally being primarily generated based on opportunistic principles. Note the extreme differences between the as-built product definition and the early in-service product definition.

## **Manufacturing process planning**

To address all restrictive inputs relevant to the entire manufacturing process workflow, the following section details secondary post-processing steps necessary for the present case study. This final step of the design process is crucial for the creation of a component suited to mass production and functionality in service. The specific steps and the ordering of these steps is part and process-specific, as discussed in the introduction.

### *Heat treatment, surface finishing, and build plate separation*

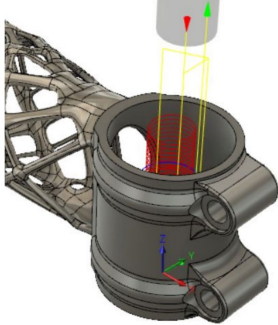
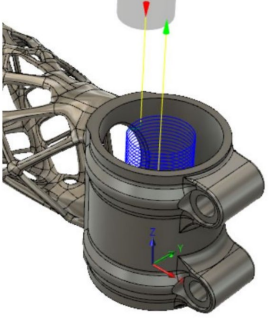
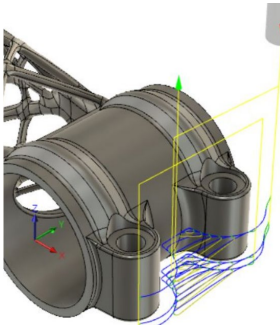
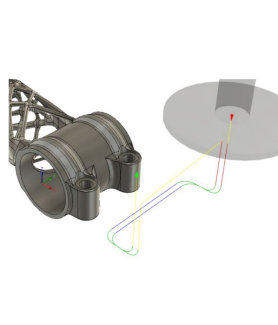
After printing, loose powder removal will be accomplished using a combination of industrial vacuuming and manual cleaning. Due to the lack of enclosed or tight spaces more rigorous methods of powder removal such as ultrasonic cleaning should not be necessary. Following powder removal, heat treatment can commence. Heat treatment is required for the bicycle stem part for two reasons: 1) to remove residual stresses induced by the rapid heating and cooling cycles innate to the LPBF process, and 2) to promote phase transformation and precipitation to produce optimal material strength. Heat treatment is to be performed on the build plate due to the restraint it offers against residual stresses. Removing the workpiece prior to a stress relief operation will lead to deformation. The prescribed heat treat is a two-part process as follows and was informed by AMS 2801BC. First, the parts are to be solutionized for 15 min at 955C (1750 F), then water quenched. This temperature is well over the static recrystallization temperature for Ti64 and will allow for stress relieve. Quenching will transform much of the high temperature microstructure to an alpha-prime martensitic phase, which will strengthen the alloy. After the part has been quenched, an aging treatment at 482 C (900 F) for 8 hours is prescribed, followed by air cooling. This intermediate temperature tempers unstable martensite and will precipitate fine beta particles, strengthening the material via precipitation hardening. Lastly, bead blasting is needed to remove scale, partially fused satellite particles, and to provide a more uniform and smoother surface finish on the stems. After heat treat the part is removed from the build plate. Due to the solid volume support connecting the part to the build plate, a low-precision high speed approach is viable. Band sawing will be used, as this is a more cost effective and faster method than wire-EDM.

### *Finish-machining*

A bicycle stem has several features that require precise dimensional control and good surface finish not within the capabilities of LPBF. These features include the bore mating surfaces that clamp the stem to the steerer tube and the handlebars. To clamp these with evenly distributed pressure that does not unduly stress the stem, the internal diameter of the bore must be controlled with tight tolerance. Additionally, high surface roughness can damage the clamped steerer tube

and handlebars. A machining process was developed for use with a two-station vise on a 3+1 axis or higher degree of freedom vertical machining center. The overall process requires two set-ups. To appropriately hold the bicycle stem, two pairs of ‘soft jaws’ that conform to the as-built outer profile of the handlebar and steerer tube mounts will be manufactured for each of the two work-holding stations. In the first set-up the steerer tube clamp is fixtured in soft jaws so that it is rigidly fixtured, and the handlebar clamp is cantilevered and therefore not rigid. Thus, the second station reverses the part, fixturing the handlebar mount so that it may be machined. Five distinct operations are shown and summarized in Table 3 for the steerer tube mount side of the stem. Similar operations are performed on the handlebar mount side except for the build plate support removal. In summary, the bulk of machining allowances within the bore are first removed using an adaptive clearing strategy. Then, finish boring is performed with small depth of cuts to create a precise, high surface finish bore. Next the build plate support is machined away using an adaptive clearing strategy and bolt holes are drilled and tapped. Finally, a slitting operation is performed so that the mount may properly clamp the steerer tube or handlebars when the pinch bolts are tightened. This operation requires a plug for the machined bore to ensure no deformation under fixturing loads while machining.

*Table 3. Machining process plan overview*

<b>Operation 1</b>	<b>Operation 2</b>	<b>Operation 3 &amp; 4</b>	<b>Operation 5</b>
Rough milling of bore	Finish boring	Removal of support, drilling and tapping of holes	Slitting
5 min, 34 sec	6 min, 23 sec	1 min, 15 sec	6 min, 8 sec
			

### Technical evaluation

To evaluate the technical fitness of the design, a static finite element (FE) model was created using Abaqus/CAE to evaluate the stress distribution experienced by the bicycle stem during the four examined loading scenarios. Although the FE model cannot validate the design entirely or itself be validated without experimental testing not performed for this case study, it can still be useful as a secondary check of the generative design tool output. Acknowledging these limitations, the details of the modeling approach are provided below.

Boundary conditions were applied to the bicycle stem model in a similar manner to the GD tool. However, due to slight differences in the GD and FE tools, a reference point in the center of the handlebar mount was defined and rigidly constrained to exist at the center of the bore during the small deformations occurring due to loading. Either a point force or point moment is applied

to the reference point depending on the loading case, which simulated application of loading conditions detailed in Table 1. All translations and rotations of the steerer tube mount were constrained to fix the model in space and simulate a fixed steerer tube mount.

The model was meshed using C3D10 quadratic tetrahedral elements with a mesh size of 0.2 mm. A mesh convergence study, not shown here for brevity, was performed, and verified that this mesh size is sufficiently fine to capture the bulk stress-strain response of the bicycle stem under the specified loading conditions. Analysis of the four loading scenarios revealed that the R tool produced a design that with stress distributions consistent with design specifications. Figure 7 shows the resulting stress distributions along on the deformed geometry for each loading scenario. Note that deformations are exaggerated for visual effect. As can be seen in this figure, particularly in the “starting” scenarios, which represent the most severe loads observed by the bicycle stem, the stress distribution is uniform throughout the GD-optimized region. This can be seen by the consistent green stress value within this region.

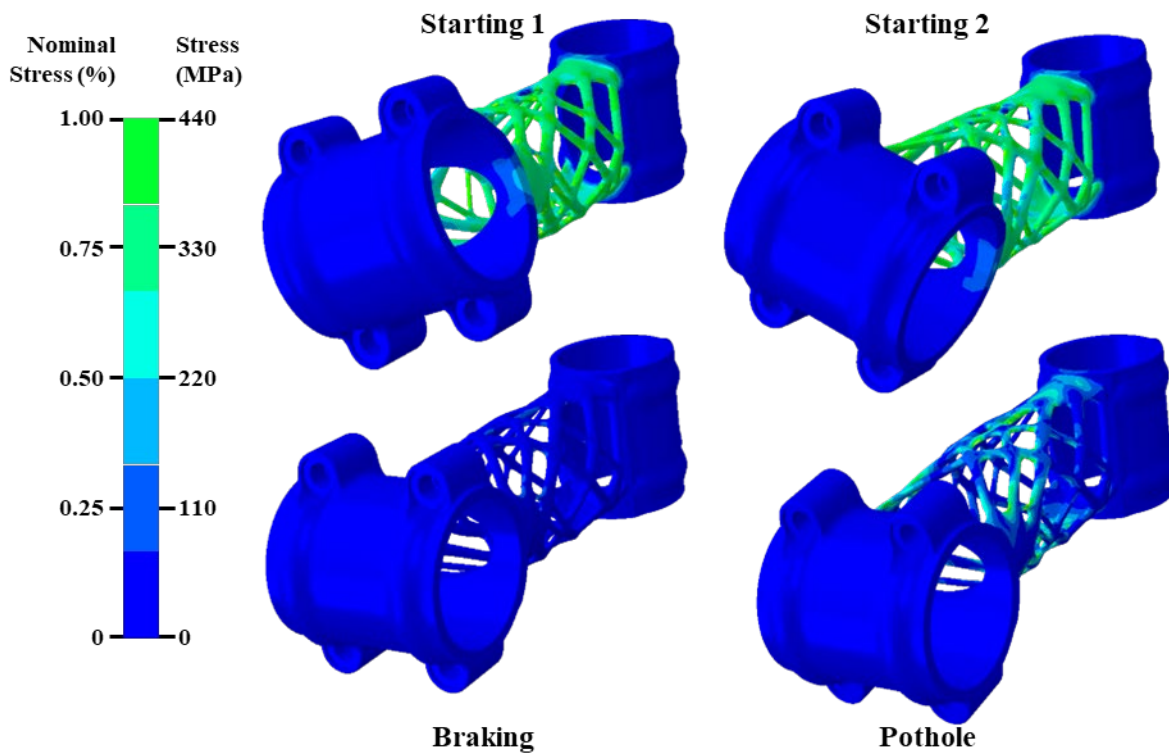


Figure 7. Finite element model results showing nominal stress distributions in samples. Deformations exaggerated for visual effect.

### Conclusions

In the case study presented above, a bicycle stem was redesigned for AM with significant weight savings as a major result. The resulting weight reduction from 190 g to 140 g represents a 26% weight reduction. The presented case study exemplifies the intermediate role of design optimization tools that take advantage of AM design freedom, such as generative design in the present case. A key takeaway is that while GD might produce a design feasible to manufacture

using an AM process, additional work, notably a rigorous and encompassing DFAM study, is required. Numerous practical challenges for the AM process and the subsequent manufacturing workflow persist which must be considered for a successful redesign. As with any redesign, a thorough economic analysis would be required to fully evaluate whether the weight savings realized through generative redesign are economically worthwhile. Although such an analysis is beyond the scope of the present work, the significant weight savings demonstrate the capacity of generative design to redesign light-weighted components.

Specifically, the GD tool utilized in this work includes DFAM heuristics limited to build orientation, allowable overhang angle, and minimum feature size. However, as demonstrated in the examined case study, further considerations were necessary to fully prepare a design for the manufacturing process. Human intervention in the design process resulted in numerous other heuristics levied against the early embodiment designs, ultimately improving the product. For example, DFAM heuristics were used to remove unbuildable geometry such as the large horizontal bores of the handlebar and steerer tube mounts and modify the geometry of the bolt hole bosses to avoid requiring supports. Other DFM inputs to the detail design phase were critical. Supports were designed to allow for efficient and cost-effective build plate separation. Rough, as-built surfaces were remedied after heat treatment but before machining. Machining allowances were added to critical surfaces, tool access and fixturing were considered, and order of set-ups designed. These tasks represent restrictive DFM which goes far beyond simple DFAM heuristics and is based in a detailed consideration of the entire manufacturing workflow.

In summary, the presented case study was used to demonstrate the multitude of practical challenges that arise when designing an AM part. Specific challenges related to generative design were overcome through human intervention and design modifications. Secondary processing steps were identified during the design process and modifications to the design were made to fluidly incorporate these steps. Through consideration of the restrictions and requirements of the necessary manufacturing processes throughout the entire manufacturing workflow, design modifications were made to improve the manufacturability of the proposed design.

### **References**

- [1] D.W. Rosen, Research supporting principles for design for additive manufacturing, *Null*, 9 (2014) 225–232. <https://doi.org/10.1080/17452759.2014.951530>.
- [2] C.C. Seepersad, Challenges and Opportunities in Design for Additive Manufacturing, *3D Printing and Additive Manufacturing*, 1 (2014) 10–13. <https://doi.org/10.1089/3dp.2013.0006>.
- [3] A.R. Mashhadi, B. Esmaeilian, S. Behdad, Impact of Additive Manufacturing Adoption on Future of Supply Chains, in: *MSEC2015, Volume 1: Processing*, 2015. <https://doi.org/10.1115/MSEC2015-9392>.
- [4] M. Fera, R. Macchiaroli, F. Fruggiero, A. Lambiase, A new perspective for production process analysis using additive manufacturing—complexity vs production volume, *The International Journal of Advanced Manufacturing Technology*, 95 (2018) 673–685. <https://doi.org/10.1007/s00170-017-1221-1>.

- [5] F. Laverne, F. Segonds, N. Anwer, M. Le Coq, Assembly Based Methods to Support Product Innovation in Design for Additive Manufacturing: An Exploratory Case Study, *Journal of Mechanical Design*. 137 (2015). <https://doi.org/10.1115/1.4031589>.
- [6] N.A. Meisel, M.R. Woods, T.W. Simpson, C.J. Dickman, Redesigning a Reaction Control Thruster for Metal-Based Additive Manufacturing: A Case Study in Design for Additive Manufacturing, *Journal of Mechanical Design*. 139 (2017). <https://doi.org/10.1115/1.4037250>.
- [7] S. Hällgren, L. Pejryd, J. Ekengren, (Re)Design for Additive Manufacturing, *Procedia CIRP*. 50 (2016) 246–251. <https://doi.org/10.1016/j.procir.2016.04.150>.
- [8] T. Briard, F. Segonds, N. Zamariola, G-DfAM: a methodological proposal of generative design for additive manufacturing in the automotive industry, *International Journal on Interactive Design and Manufacturing (IJIDeM)*. 14 (2020) 875–886. <https://doi.org/10.1007/s12008-020-00669-6>.
- [9] A. Wiberg, J. Persson, J. Ölvander, Design for additive manufacturing – a review of available design methods and software, *Rapid Prototyping Journal*. 25 (2019) 1080–1094. <https://doi.org/10.1108/RPJ-10-2018-0262>.
- [10] T. Zegard, G.H. Paulino, Bridging topology optimization and additive manufacturing, *Structural and Multidisciplinary Optimization*. 53 (2016) 175–192. <https://doi.org/10.1007/s00158-015-1274-4>.
- [11] S.N. Reddy K., I. Ferguson, M. Frecker, T.W. Simpson, C.J. Dickman, Topology Optimization Software for Additive Manufacturing: A Review of Current Capabilities and a Real-World Example, in: *IDETC-CIE2016, Volume 2A: 42nd Design Automation Conference, 2016*. <https://doi.org/10.1115/DETC2016-59718>.
- [12] J. ZHU, H. ZHOU, C. WANG, L. ZHOU, S. YUAN, W. ZHANG, A review of topology optimization for additive manufacturing: Status and challenges, *Chinese Journal of Aeronautics*. 34 (2021) 91–110. <https://doi.org/10.1016/j.cja.2020.09.020>.
- [13] R. Willner, S. Lender, A. Ihl, C. Wilsnack, S. Gruber, A. Brandão, L. Pambaguian, M. Riede, E. López, F. Brueckner, C. Leyens, Potential and challenges of additive manufacturing for topology optimized spacecraft structures, *Journal of Laser Applications*. 32 (2020) 032012. <https://doi.org/10.2351/7.0000111>.
- [14] J. Wu, X. Qian, M.Y. Wang, Advances in generative design, *Computer-Aided Design*. 116 (2019) 102733. <https://doi.org/10.1016/j.cad.2019.102733>.
- [15] J. Jiang, Y. Xiong, Z. Zhang, D.W. Rosen, Machine learning integrated design for additive manufacturing, *Journal of Intelligent Manufacturing*. 33 (2022) 1073–1086. <https://doi.org/10.1007/s10845-020-01715-6>.
- [16] X. Peng, L. Kong, J.Y.H. Fuh, H. Wang, A Review of Post-Processing Technologies in Additive Manufacturing, *JMMP*. 5 (2021) 38. <https://doi.org/10.3390/jmmp5020038>.
- [17] J. Berez, C. Saldana, Fatigue of laser powder bed fusion processed 17-4 stainless steel using prior process exposed powder feedstock, *Journal of Manufacturing Processes*. 71 (2021) 515–527. <https://doi.org/10.1016/j.jmapro.2021.09.045>.
- [18] A. Soltani-Tehrani, J. Pegues, N. Shamsaei, Fatigue behavior of additively manufactured 17-4 PH stainless steel: The effects of part location and powder re-use, *Additive Manufacturing*. 36 (2020) 101398. <https://doi.org/10.1016/j.addma.2020.101398>.
- [19] P.D. Nezhadfar, K. Anderson-Wedge, S.R. Daniewicz, N. Phan, S. Shao, N. Shamsaei, Improved high cycle fatigue performance of additively manufactured 17-4 PH stainless steel

- via in-process refining micro-/defect-structure, *Additive Manufacturing*. 36 (2020) 101604. <https://doi.org/10.1016/j.addma.2020.101604>.
- [20] A. Yadollahi, M. Mahmoudi, A. Elwany, H. Doude, L. Bian, J.C. Newman, Fatigue-life prediction of additively manufactured material: Effects of heat treatment and build orientation, *Fatigue Fract Eng Mater Struct*. 43 (2020) 831–844. <https://doi.org/10.1111/ffe.13200>.
- [21] P.D. Nezhadfar, R. Shrestha, N. Phan, N. Shamsaei, Fatigue behavior of additively manufactured 17-4 PH stainless steel: Synergistic effects of surface roughness and heat treatment, *International Journal of Fatigue*. 124 (2019) 188–204. <https://doi.org/10.1016/j.ijfatigue.2019.02.039>.
- [22] M. Ahlfors, Hot Isostatic Pressing for Metal Additive Manufacturing, in: D.L. Bourell, W. Frazier, H. Kuhn, M. Seifi (Eds.), *Additive Manufacturing Processes*, ASM International, 2020: pp. 316–323. <https://doi.org/10.31399/asm.hb.v24.a0006552>.
- [23] T. Persenot, G. Martin, R. Dendievel, J.-Y. Buffière, E. Maire, Enhancing the tensile properties of EBM as-built thin parts: Effect of HIP and chemical etching, *Materials Characterization*. 143 (2018) 82–93. <https://doi.org/10.1016/j.matchar.2018.01.035>.
- [24] A. du Plessis, E. Macdonald, Hot isostatic pressing in metal additive manufacturing: X-ray tomography reveals details of pore closure, *Additive Manufacturing*. 34 (2020) 101191. <https://doi.org/10.1016/j.addma.2020.101191>.
- [25] J. Elambasseril, J. Rogers, C. Wallbrink, D. Munk, M. Leary, M. Qian, Laser powder bed fusion additive manufacturing (LPBF-AM): the influence of design features and LPBF variables on surface topography and effect on fatigue properties, *Null*. (2022) 1–37. <https://doi.org/10.1080/10408436.2022.2041396>.
- [26] S. Detwiler, D. Watring, A. Spear, B. Raeymaekers, Relating the surface topography of as-built Inconel 718 surfaces to laser powder bed fusion process parameters using multivariate regression analysis, *Precision Engineering*. 74 (2022) 303–315. <https://doi.org/10.1016/j.precisioneng.2021.12.003>.
- [27] M. Yonehara, C. Kato, T.-T. Ikeshoji, K. Takeshita, H. Kyogoku, Correlation between surface texture and internal defects in laser powder-bed fusion additive manufacturing, *Sci Rep*. 11 (2021) 22874. <https://doi.org/10.1038/s41598-021-02240-z>.
- [28] J.C. Fox, S.P. Moylan, B.M. Lane, Effect of Process Parameters on the Surface Roughness of Overhanging Structures in Laser Powder Bed Fusion Additive Manufacturing, *Procedia CIRP*. 45 (2016) 131–134. <https://doi.org/10.1016/j.procir.2016.02.347>.
- [29] B.H. Jared, M.A. Aguilo, L.L. Beghini, B.L. Boyce, B.W. Clark, A. Cook, B.J. Kaehr, J. Robbins, *Additive Manufacturing: Toward Holistic Design*, *Scripta Materialia*. 135 (2017) 141–147. <https://doi.org/10.1016/j.scriptamat.2017.02.029>.
- [30] S. Yang, Y.F. Zhao, Additive manufacturing-enabled design theory and methodology: a critical review, *The International Journal of Advanced Manufacturing Technology*. 80 (2015) 327–342. <https://doi.org/10.1007/s00170-015-6994-5>.
- [31] L.L. Lopez Taborda, H. Maury, J. Pacheco, Design for additive manufacturing: a comprehensive review of the tendencies and limitations of methodologies, *Rapid Prototyping Journal*. 27 (2021) 918–966. <https://doi.org/10.1108/RPJ-11-2019-0296>.
- [32] R.K. Leach, D. Bourell, S. Carmignato, A. Donmez, N. Senin, W. Dewulf, Geometrical metrology for metal additive manufacturing, *CIRP Annals*. (2019) 1–24. <https://doi.org/10.1016/j.cirp.2019.05.004>.

- [33] A. Townsend, L. Pagani, L. Blunt, P.J. Scott, X. Jiang, Factors affecting the accuracy of areal surface texture data extraction from X-ray CT, *CIRP Annals*. 66 (2017) 547–550. <https://doi.org/10.1016/j.cirp.2017.04.074>.
- [34] M. Seifi, A. Salem, J. Beuth, O. Harrysson, J.J. Lewandowski, Overview of Materials Qualification Needs for Metal Additive Manufacturing, *JOM*. 68 (2016) 747–764. <https://doi.org/10.1007/s11837-015-1810-0>.
- [35] F.H. Kim, S.P. Moylan, Literature review of metal additive manufacturing defects, National Institute of Standards and Technology, Gaithersburg, MD, 2018. <https://doi.org/10.6028/NIST.AMS.100-16>.
- [36] G.E. Dieter, L.C. Schmidt, *Engineering Design*, 5th ed., McGraw-Hill, New York, NY, 2013.
- [37] A. Yadollahi, N. Shamsaei, Additive manufacturing of fatigue resistant materials: Challenges and opportunities, *International Journal of Fatigue*. 98 (2017) 14–31. <https://doi.org/10.1016/j.ijfatigue.2017.01.001>.
- [38] B. Blakey-Milner, P. Gradl, G. Snedden, M. Brooks, J. Pitot, E. Lopez, M. Leary, F. Berto, A. du Plessis, Metal additive manufacturing in aerospace: A review, *Materials & Design*. 209 (2021) 110008. <https://doi.org/10.1016/j.matdes.2021.110008>.
- [39] D. Bourell, J.P. Kruth, M. Leu, G. Levy, D. Rosen, A.M. Beese, A. Clare, Materials for additive manufacturing, *CIRP Annals*. 66 (2017) 659–681. <https://doi.org/10.1016/j.cirp.2017.05.009>.
- [40] P.D. Soden, B.A. Adeyefa, Forces applied to a bicycle during normal cycling, *Journal of Biomechanics*. 12 (1979) 527–541. [https://doi.org/10.1016/0021-9290\(79\)90041-1](https://doi.org/10.1016/0021-9290(79)90041-1).
- [41] D. Covill, P. Allard, J.-M. Drouet, N. Emerson, An Assessment of Bicycle Frame Behaviour under Various Load Conditions Using Numerical Simulations, *Procedia Engineering*. 147 (2016) 665–670. <https://doi.org/10.1016/j.proeng.2016.06.269>.